



Colloidal Quantum Wells for Optoelectronic Devices

Journal:	<i>Journal of Materials Chemistry C</i>
Manuscript ID	TC-REV-03-2020-001164.R1
Article Type:	Review Article
Date Submitted by the Author:	30-Mar-2020
Complete List of Authors:	Diroll, Benjamin; Argonne National Laboratory, Center for Nanoscale Materials

Review

Colloidal Quantum Wells for Optoelectronic Devices

Benjamin T. Diroll^{a*}Received 00th January 20xx,
Accepted 00th January 20xx

DOI: 10.1039/x0xx00000x

Colloidal quantum wells, also called nanoplatelets, are nanoscopic materials displaying quantum confinement in two dimensions. Unlike colloidal quantum dots, colloidal quantum well ensembles have no inhomogeneous broadening due to an atomically-precise definition of the short axis, a fact which results in much narrower ensemble absorption and emission. Thus, colloidal quantum wells can translate many advantages of colloidal nanocrystals or other solution-processable materials, such as scalable synthesis and substrate-agnostic deposition (particularly compared to epitaxial quantum wells), without sacrificing material uniformity. Due to very narrow photoluminescence peaks, these materials have found a home in applications involving light emission, such as downconversion enhancement films, light-emitting diodes, and lasers, in which they represent some of the best performers among solution-cast materials. As argued in this review, the full spectrum of epitaxial quantum well devices offers a roadmap to other potential applications, such as detection, electronics, electro-optics, non-linear optics, or intersubband devices, in which only nascent efforts have been made.

1 Introduction

Colloidal quantum wells (CQWs), commonly called nanoplatelets, are atomically-precise materials with two-dimensional quantum confinement. The physics of these materials mirrors more commonly studied epitaxial quantum wells,¹ but they are synthesized in organic solvents at modest temperatures (normally 100-300 °C). Despite variable long dimensions, the atomically-precise thickness of the CQWs places these materials in a distinct class from other colloidal nanocrystals: except at the very smallest lateral sizes, their band gaps are not influenced by lateral size dispersion and the optical spectra of CQWs are thermally-limited. CQWs lift synthetic constraints of epitaxial materials, particularly the disadvantages of costly synthesis on specialized substrates at high temperatures and low pressures. CQW may be processed in solution by techniques such as spray-coating, spin-coating, inkjet printing, layer-by-layer, or imprint lithography and deposited on to substrates of arbitrary composition and shape. At the same time, they retain the electronic structure of quantum wells and thermally-limited optical resonances which are advantageous in many applications.

This review is focused chiefly on the applications of II-VI CQWs, especially those to which they are uniquely well-suited. From a technological perspective, epitaxial quantum wells provide a useful atlas of possible applications for colloidal cousins which is followed here. The development of epitaxial quantum wells drove substantial improvements or completely new technologies in both large-scale and niche applications in displays, lasers, nonlinear optics, electronics, and detectors. Earlier works have extensively reviewed the preparation of

CQWs and synthetic work will only be described in here to provide a foundation for device applications. Subsequent sections in this review will focus on the applications for CQW emission, linear absorption, non-linear properties, and intersubband applications. Although some of these areas are already subject to intense study, other topics covered in this review have been left largely unexamined despite the success of epitaxial quantum wells in similar applications.

2 Composition and Structure of Colloidal Quantum Wells and their Assemblies

Presently, high purity syntheses of CQWs are limited to II-VI semiconductor materials, with CdSe the most common. Previous works have reviewed much of this chemistry²⁻⁵ and it will not be addressed in detail here. Synthetic routes to monodisperse materials exist for CdS, CdS_{1-x}Se_x, CdSe, CdTe, HgSe, HgTe, ZnS, ZnSe, and PbS, as well as doped-CQW structures (See Table 1).^{1,6-10} Although commonly discussed as zinc blende (cubic) polymorphs, X-ray diffraction shows that these materials are actually tetragonal.¹¹ Collectively, these materials have absorption edges spanning the ultraviolet to the near-infrared. Examples of monodisperse CdS, CdSe, and CdTe CQW ensemble absorption shown in Figure 1a span thicknesses from 5 atomic layers (2.5 monolayers of CdE) to 13 atomic layers (6.5 ML). Although a typical size of the CQW lateral dimensions is less than 100 nm, growth over larger dimensions is possible through continuous injection akin to living polymerization.¹² Control over lateral aspect ratios can also be achieved by adjusting the proportion of short carboxylic acids in the reaction mixture.¹³

Core/shell CQWs come in at least two types, shown in Figure 1b. Core-crown structures have a shell grown exclusively along the long axes of the CQW, which have optical absorption similar

^a Center for Nanoscale Materials, Argonne National Laboratory, Lemont, IL 60439, United States. E-mail: bdiroll@anl.gov

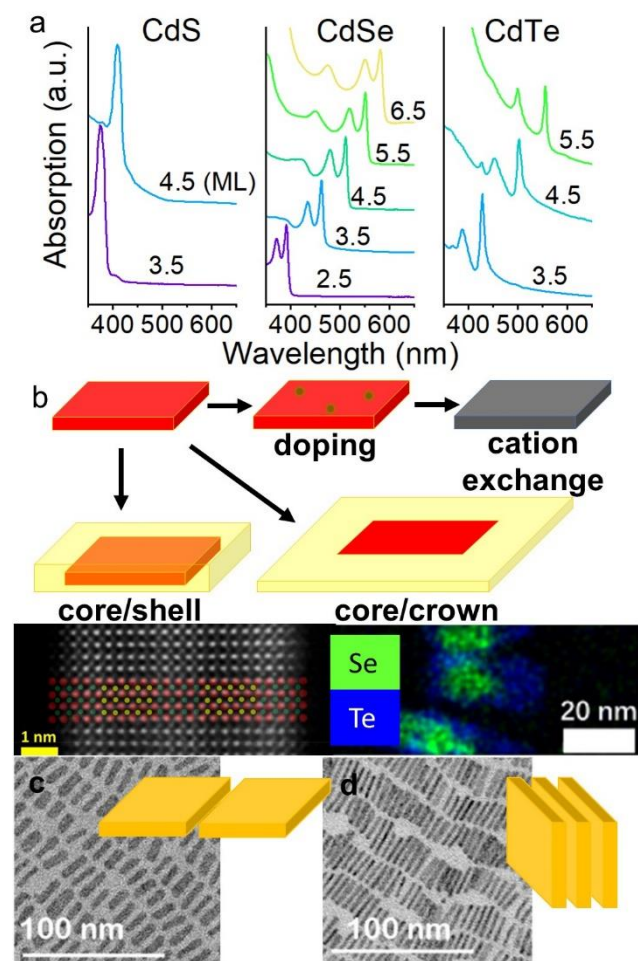


Figure 1. (a) Absorption spectra of CdS, CdSe, and CdTe CQWs. Thicknesses are asserted based upon literature findings. (b) Routes to composition variation through cation exchange and core/shells. Below the core/shells are a micrograph (left) of CdSe/CdS/CdSe/CdS/CdSe atomically-precise core/shell and (right) elementally-mapped CdSe/CdTe type-II core/crown structures. Reproduced from Refs. 16 and 110 with permission from the American Chemical Society. (c, d) Large-area alignment of CQW films in face-down and edge-down geometries, respectively. Reproduced from Ref. 26 with permission from the American Chemical Society.

to isolated CQWs and may be type I (e.g. CdSe/CdS) or type II (e.g. CdSe/CdTe).¹⁴ Isotropic core/shell structures can be grown with preserved atomic precision through methods like colloidal atomic layer deposition^{15,16} or, without atomic precision, by familiar secondary shell growth protocols involving slow secondary injection.^{17–19} Both may be combined as well.²⁰

An important distinction from epitaxial wells is that CQWs are symmetric on both top and bottom faces. CQWs comprise an odd number of atomic layers in total. Combined with revisions of the thickness labels of early reports, this has led to some confusion in sample labelling. Here, the number of metal chalcogenide layers will be used: for example, samples with 7 total atomic layers will be described as “3.5 monolayers” (e.g. 3.5 ML CdSe), although in the literature “3 monolayers” is frequently used. Less trivially, the symmetrical termination of CQWs makes them strain balanced, which can be challenging to achieve in epitaxial systems and reduces bandwidth of optical resonances arising from strain heterogeneity.²¹

Compared to quantum dots, a limitation cited for CQWs is that tunability in optical or electronic properties is lost. For example, CdSe CQWs may be synthesized for room temperature emission at 463 nm, 514 nm, or 553 nm, but not in between. This is a false choice, and not only because of tuning achievable with alloys or core/shell structures. Several works have shown that and that control of the CQW thickness (and therefore electronic structure) can be achieved at a resolution better than one atomic layer by ligand-induced changes in the CQW lattice.^{22–24} Replacing carboxylic acid ligands with thiolates, phosphonates, or halide ligands expands the tetragonal lattice of CQWs in the short axis dimension, relaxing confinement. An appropriate choice of ligand chemistry tunes the band gap of CdSe CQWs across visible wavelengths.

Another point critical to device performance is the control over the alignment of CQWs. In most of the devices described below, there is no purposeful control over the structure of CQW layers, although they are known to form assemblies of stacked plates. Linear alignment of CQWs has been achieved with samples in polymers with stretching²⁵ or by deposition on to liquid interfaces, as shown in Figures 1c and 1d.²⁶ Electrophoretic separation strongly implies that CQWs have a permanent dipole and thus may be aligned in electric fields as well.²⁷ Alternatively, unstacked, face-down CQWs can be achieved with ligand chemistry and directed assembly.²⁸ Dispersed helical superstructures displaying circular dichroism have been formed through various ligand-exchange reactions²⁹ and linear lamellar structures show emergent optical polarization.³⁰ Substantial interactions between co-facial CQWs in particular has been demonstrated in highly-efficient Förster resonant energy transfer (FRET)^{31,32} or the possibility of excimer or miniband formation.^{33,34} In applications in which polarization control or interfacial interactions are consequential, alignment or turbostratic disorder of CQW solids will impact performance. Hierarchical order, including placement on pre-fabricated structures like photonic crystals can obviously affect device performance, but these effects are not intrinsic to CQWs.^{28,35,36}

Table 1. Properties of Known Core-only Colloidal Quantum Wells

Type	Monolayers	λ_{abs} (nm)	Notes
CdS	2.5-5.5	326-427	2.5, 5.5 polydisperse ¹
CdSe	2.5-8.5	397-622	>6.5 impurities ³⁷
CdTe	3.5-5.5	428-556	>5.5 polydisperse ¹
ZnS	4.5	325	cation exchange ⁶
ZnSe	4.5	411	core/Shell cation exchange ⁶
HgSe	3.5	766	cation exchange ⁷
HgTe	3.5	880	cation exchange ⁷

3 Photoluminescence Applications

A Enhancement Films

The narrow photoluminescence of CQWs, compared to other colloidal nanocrystal systems or organic dyes, stimulated interest in applying CQWs for light-emitting applications. Enhancement films, which convert a blue excitation into red and green colours for displays, require the mutual optimization of

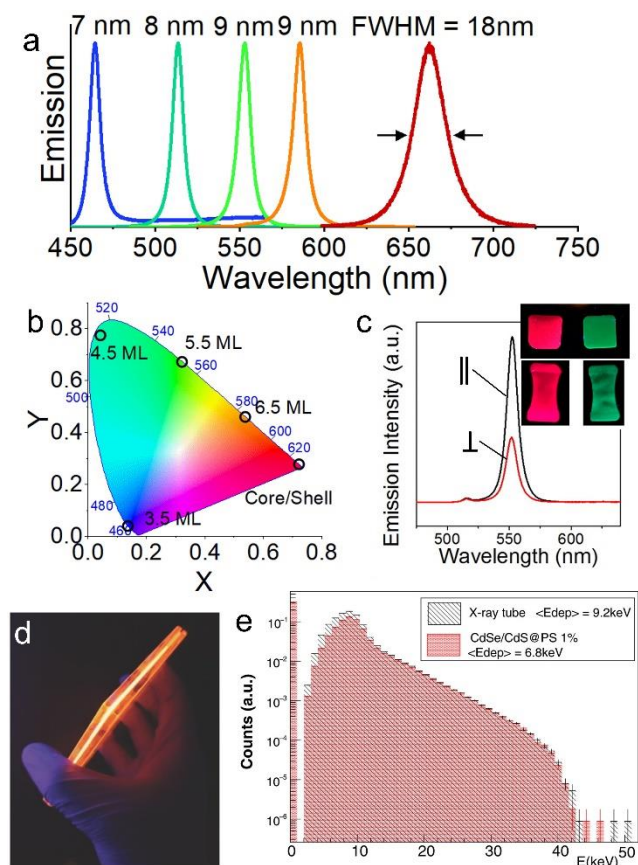


Figure 2. (a) Room temperature photoluminescence spectra of 3.5 ML, 4.5 ML, 5.5 ML, 6.5 ML CdSe CQW ensembles, and 4 ML CdSe/4 ML CdS core/shell CQWs. The full-width at half maximum for each sample is labelled on the plot. (b) Placement of room temperature CdSe CQW emission spectra on the CIE colour space. (c) Polarization-resolved emission of CQWs embedded in stretched polymer, with the inset image showing the unstretched and stretched polymers containing core/shell and core-only CQWs under ultraviolet illumination. Reproduced from Ref. 25 with permission from the American Chemical Society. (d) Luminescent solar concentrator made with Cu-doped CdSe CQWs. Reproduced from Ref. 10 with permission from Wiley. (e) Emission counts for CQW scintillator under X-ray illumination of variable energy. Reproduced from Ref. 66 with permission from Nature Publishing Group.

emission wavelength, bandwidth, stability, and quantum yield. CQWs have been demonstrated in enhancement films in which the CQWs are embedded in a polymer or copolymer matrix.^{25,38–40} The chief advantage of CQWs is their narrow ensemble emission (Figure 2a), which resembles that of isolated CQWs.⁴¹ If the narrow emission of CQWs (8 nm in blue; 10 nm in green; < 20 nm in red) is preserved, they enable spanning nearly the full color gamut. As shown in Figure 2b, emission from CdSe CQWs decorates the edges of colour space defined by the Commission internationale de l'éclairage (CIE) coordinates.

Many of the same advantages of inorganic nanocrystals for downconversion, such as durability and bright emission, should be available to CQWs but synthetic challenges remain to achieve them. Efficient emission is a necessity and the synthetic quality of materials, particularly of core/shell CQWs, is improving quantum yields to near unity. As-synthesized, the quantum yield of green-emitting CdSe core-only CQWs can reach ~50%,⁴² with blue-emitting CdSe, CdTe, and CdS samples showing poorer efficiencies of < 10%, typically.^{9,43} As with quantum dots, core/shell growth improves quantum yields.

Core/crown CdSe/CdS and CdSe/CdTe have quantum yields 60%⁴⁴ to 70–85%,^{45–47} respectively. The type I CdSe/CdS core/crown geometry is particularly advantageous because it largely preserves the colour (and bandwidth) of the initial core emission. For red emission, high-temperature core/shell formation via annealed colloidal ALD processes, which preserves atomic precision and linewidths as narrow as 16 nm, produce samples with 80% quantum yields. Quantum yields as high as 95% are reported for slow secondary injection methods to form CdSe/Cd_xZn_{1-x}S.⁴⁸ Combinations of CdSe/CdS core/crown with isotropic ZnS shells are also reported with quantum yields as high as 90%.²⁸

An additional advantage of CQWs is that they emit light which is polarized in the wide plane of the CQW.^{25,49} Controlled emission polarization improves the efficiency of display operation and simplifies construction. Indeed, CQWs have been demonstrated in stretched enhancement films as in Figure 2c, which preferentially align the CQWs with the stretching axis to enrich the polarization of emission.^{25,39,50} Two-dimensional planar dipoles of emission suppress the peak achievable polarization compared to uniaxial dipole systems such as nanorods. However, tuning of the aspect ratio of the CQWs synthetically can yield materials with a rectangular cross-section which preferentially enhances emission along the longest-axis direction of the CQW through dielectric effects.^{51,52}

A common problem across emitters used in enhancement films (or LEDs) is that the active layer heats up during operation.⁵³ Operating temperatures depend on intensity of use and geometry, but estimates are 150 °C for enhancement films and 80–120 °C for light-emitting diodes.⁵³ Higher temperatures broaden and red-shift emission, similar to other quantum dots or bulk materials,^{54,55} but these effects are small enough that they do not diminish the appeal of CQW emitters. Preservation of emission at elevated temperatures is more challenging. Core-only CQWs show photoluminescence quenching to about 40% of room-temperature values at 120 °C,^{54,55} which is better than core-only InP or small CdSe quantum dots, but worse than most core/shell materials.^{55–59} Low-temperature shell growth did not improve stability substantially.⁵⁴ CdSe/CdZnS CQWs with shells grown at high-temperature also showed emission 40–60% weaker than room temperature values at 400 K, but with improved stability and reversibility.⁴⁸ A peculiar challenge of CQWs is that a large fraction of (thermally-reversible) photoluminescence losses at high temperature are due to activated Förster resonance energy transfer (FRET) processes;⁶⁰ designing solids without stacking may be critical to avoiding this quenching effect.

B Luminescent Solar Concentrators

Doped CQWs have been proposed for use in luminescent solar concentrators (LSCs),¹⁰ in which large (typically acrylic) panels with embedded dyes concentrate solar flux through waveguiding dye emission to a much smaller cross-section on the panel edges. The small Stokes shift of undoped CQWs makes them poor candidates for LSCs, due to re-absorption losses. But similar to work in quasi-spherical colloidal systems,⁶¹ doping CdSe CQWs with ions such as copper enables a substantial red-shift of emission originating from the dopant, while preserving the sharp band-edge absorption.¹⁰ This combination is considered ideal for LSCs.⁶² In Cu-doped CdSe CQWs, dopant emission can reach quantum yields as high as 90 %, with negligible re-absorption. Fabricated LSCs (Figure 2d) reach optical efficiencies of ~ 1.5 %, with the chief limitations arising from reduced photoluminescence quantum yield in the acrylic matrix and scattering losses.¹⁰ Polarization properties of such Cu:CdSe systems are unclear, but dielectric polarization coupled with alignment within the LSC waveguide may improve light trapping.

C Quantum Emission

One distinctive property of CQWs compared with epitaxial quantum wells is that tunable small lateral size enables a transition to a quantum emitter exhibiting anti-bunching behaviour.⁴¹ Judicious selection of the lateral size allows antibunching with a virtual absence of biexcitons to near unity yield of biexcitons.⁶³ Furthermore, multiple studies have demonstrated that CdSe CQWs show polarized emission from face-down CQWs depending on the dimensions of the CQW plane: those with rectangular cross sections are polarized by dielectric effects whereas those with square cross sections are not.^{64,65} When aligned vertically, as has been achieved in thick shell CdSe/CdS CQWs, samples show large linear polarization reflecting the projection of the large two-dimensional sample plane on to the measurement axis.⁶⁶ Although this application of CQWs is distinctive from epitaxial materials, it is similar to colloidal nanocrystals and CQWs do not necessarily overcome drawbacks of spectral wandering or blinking in unique ways.

D Scintillators for High-Energy Radiation

A small number of reports have investigated CQWs as potential scintillators.^{67–69} CQW photoluminescence occurring when samples are irradiated with X-rays, gamma rays, or electrons is used to detect the high-energy radiation indirectly (Figure 2e). The chief advantage of CQWs is their potential for high time-resolution scintillation with pulsed excitation, which is important in high-energy physics and certain medical applications. CQWs show prompt response times and are less sensitive to non-radiative Auger recombination compared to (bulk) alternatives.⁶⁹ Quantum yield, photoluminescence line-shape, and dynamics in CQWs are all influenced by high-energy radiation due to multiple exciton generation.⁷⁰ This is manifest through red-shifted, broadened, and more rapid emission from biexcitons. CQWs can already have sub-nanosecond emission at lower temperatures,^{1,71,72} but under X-ray or gamma ray irradiation, multi-exciton emission brings the functional coincidence time for CdSe CQW scintillators to 80 ps.⁶⁷

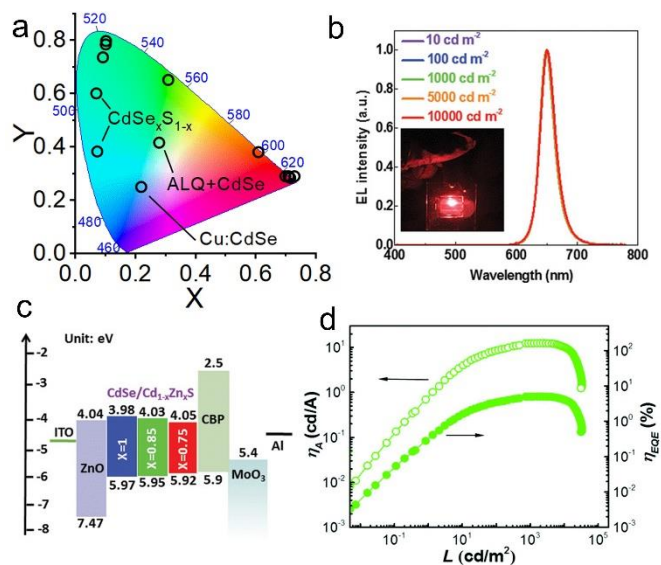


Figure 3. (a) CIE coordinate space with open circles representing reported results for CQW-based LEDs. CIE coordinates derived from published works or estimated from given centre wavelength and bandwidth information. (b) Narrow red electroluminescence is preserved over a large range of luminance for the CQW LED shown inset. (c) Inverted geometry design of a high-efficiency CQW LED. (b, c) Reproduced from Ref. 76 with permission from Wiley. (d) Efficiency roll-off of green CQW LED design. Reproduced from Ref. 77 with permission from The Royal Society of Chemistry.

4 Electroluminescent Devices

Electroluminescent devices represent a second step in complexity to leverage CQW emission for displays. Several light-emitting diodes of CQWs have been demonstrated, with saturated red and green electroluminescence well-represented in the literature.^{46,47,73–79} As with downconversion films, the chief advantage of CQWs is the spectrally-narrow electroluminescence which can be achieved, characterized by a high saturation of colour in devices. CIE coordinates of reported LEDs are shown in Figure 3a and other parameters tabulated in Table 2. Reported electroluminescence line-widths of CQW-based LEDs are 21 nm for cyan,⁷⁹ 10 nm for green,⁴⁶ and 25–30 nm for red (e.g. Figure 3b),^{75,77} which represent the narrowest emission of any solution-processed materials thus far reported.^{75,77} Deeper blue or violet LEDs based upon CQWs have not yet been reported and the relatively low quantum yields of these systems are likely to impede performance. Alternatively, CdSe CQWs doped with copper display two-color electroluminescence which is tunable with voltage.⁸⁰ Both core-only CQWs and core/shell have been used as the emissive layer in LEDs, with type I core/crown type samples preserving narrow green electroluminescence.^{46,78}

CQW-based LEDs share architecture with colloidal quantum dot LEDs, as shown in Figure 3c.⁸¹ Both normal⁷⁷ and inverted⁷⁹ geometries are known with organic^{73,74} or inorganic⁷⁷ hole- and electron-transporting layers. In many cases, no ligand-exchange chemistry is used on the CQWs^{77–79} but ligand-exchange with short-chain mercaptopropionic acid is also reported.⁷⁵ Until recently, the efficiencies of CQW LEDs lagged other nanocrystal-

based LEDs. However, recent work has demonstrated external quantum efficiencies > 19 %, which have been achieved in high-quantum yield CdSe/Cd_xZn_{1-x}S core/shell CQWs.⁷⁷ Maximum luminescence values achieved in LEDs reach > 30000 cd·m⁻² in multiple instances^{47,78} with turn-on operating voltages < 2V.⁴⁷ Underpinning most of this improved performance is improved engineering of the CQW core/shell materials which have higher photoluminescence quantum yields preserved in the solid-state films used in devices. Other benefits come from engineering charge transport layers for durability, energy alignment, and balancing of injection.⁷⁴ The use of close-packed CQW films in LEDs presents challenges relative to quantum dots due to efficient FRET. Homo-FRET quenches emission by facilitating transport to a defective ensemble members.³² The potential for funneling excitations via FRET, however, remains valuable.

Challenges remain. Blue electroluminescence has not been demonstrated yet. Peak brightness of CQW devices is lower than the exceptional record of 218800 cd·m⁻² of colloidal quantum dot films.⁸² In most devices, roll-off in efficiency occurs at higher current densities as shown in Figure 3d. Often attributed to thermal or Auger effects, CQWs should at least have advantages in this respect arising from long Auger recombination times.⁸³ Operating stability of CQW LEDs remains quite poor, although some geometries have demonstrated reasonable air-stability.⁷⁴ The longest lifetime reported thus far is estimated at 12.8 hours, through improved engineering of charge transport layers and encapsulation.⁷⁷

An area which remains for exploitation is emission dipole alignment, which can raise the external efficiency limit of an LED from ~20 % for a random distribution to ~40 % for an aligned sample. This effect is exploited extensively in organic light-emitting diodes.⁸⁴ A “face down” geometry affords plane-polarized CQW emission improved escape efficiency through reduced total internal reflection of emitted light. (In monolayers, the face-down geometry will also eliminate FRET.) Although there is no intentional control of this effect in CQW LEDs, data on the angular-dependence of electroluminescence shows deviation from Lambertian expectations which may arise from CQW alignment.⁷⁵

Table 2. Representative characteristics of reported CQW light-emitting diodes

Composition	λ/nm	V _{on}	EQE _{max} /%	L _{max} /cd·m ⁻²
CdSe _x S _{1-x} ⁷⁹	496-520	<2.5	--	100
CdSe/CdS core/crown ⁷⁸	556	2.25	5.0	33000
CdSe/CdS core/crown ⁴⁶	516	2.96	0.32	1096
CdSe ⁸⁰	~515	2.1	0.016	210
Cu:CdSe ⁸⁰	broad	2.4	0.146	1153
CdSe/CdZnS ⁷⁵	645	4.7	0.63	4499
CdSe/CdZnS ⁷⁴	658	4.0	8.39	--
CdSe/CdZnS ⁷⁷	618-650	2.4-2.6	19.2	23490

5 Amplified Spontaneous Emission and Lasing

A Demonstrations of Amplified Spontaneous Emission and Lasing

Epitaxial quantum wells have been studied as laser materials for nearly 40 years⁸⁵ and CQWs demonstrate excellent performance in applications related to optical gain and lasing. Also reviewed elsewhere,^{4,86} the chief advantages of CQWs in this application, compared to colloidal quantum dots, are their larger cross sections (>10⁻¹⁴ cm² at pump wavelengths), the narrow density of states conferred by atomic precision, and slow Auger relaxation times, which may be hundreds of picoseconds. Although typically not stated CQWs, also have rapid intraband relaxation^{87,88} and moderate or slow radiative lifetimes (1 ns or longer at room temperature) which permit population inversion.¹

These advantages result in wide gain bandwidth,⁸⁹ low thresholds,^{42,89-91} and large modal gain coefficients.⁹² The fluence thresholds for ASE of CQWs under femtosecond excitation are as little as one-tenth of the threshold fluence of the best examples of colloidal quantum dot materials.⁹³ Core/shell and core-only CdSe CQWs display amplified spontaneous emission (ASE) spanning blue to red wavelengths with thresholds, under femtosecond excitation, as low as 2.5 μJ·cm⁻².^{19,42,45,89-91} Typical ASE spectra for CdSe CQWs are shown in Figures 4a and 4b. Low thresholds for multiphoton pumping have also been observed, which is likely related to the large two-photon cross section of CQWs (see section on Non-Linear Optics).^{90,94} CdS CQWs extend this spectrally into the violet, albeit with higher thresholds (< 250 μJ·cm⁻² for core-only ASE),⁴³ and alloyed systems permit tunability through the visible.⁹⁵ Although HgE CQWs are known with NIR emission, ASE has yet to be demonstrated. It is valuable to note that modestly low ASE thresholds are still possible in CQW systems with low photoluminescence quantum yields because ASE may occur faster than nonradiative channels which otherwise quench emission.

In addition to these low thresholds for ASE, CQWs also display high modal gain coefficients, which measure how much light is amplified in a material per unit distance. Reported gain coefficients for CdSe CQW solids reach 6600 cm⁻¹,⁹² determined using the stripe-length method.⁹⁶ Other methods suggest modal gain as large as 15000 cm⁻¹.⁹⁷ For context, this is much greater than quantum dots (normally < 200 cm⁻¹),⁹⁸ larger than any other reported material at room temperature, and greater than modal gain in bulk CdSe (1000 cm⁻¹) even at 2 K.⁹⁹ An important note, however, is that although measures of fluence threshold or gain coefficients are indicative of an excellent gain medium, these numbers are strongly effected by film quality (e.g. scattering) and are not intrinsic to the materials. Further reduction in ASE thresholds or increases in gain coefficients are possible with better understanding or control of CQW solids.

The advantages of CdE CQWs as gain media have been leveraged to develop lasers, initially with femtosecond pulses, but subsequently extended to continuous wave operation. At least three laser geometries have been employed: vertical cavities, whispering galleries, and photonic crystals. The

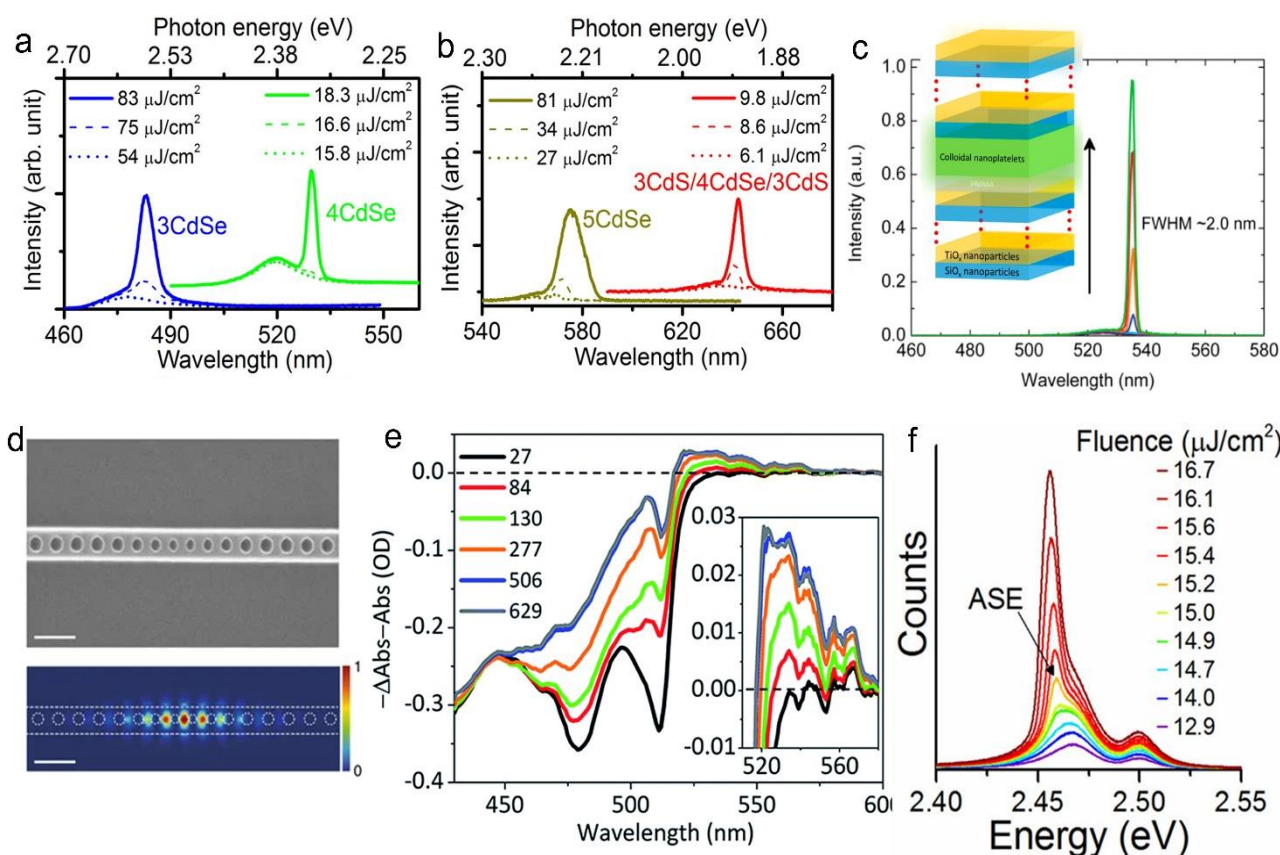


Figure 4. (a, b) Emission spectra of 3.5, 4.5, 5.5 ML CdSe CQWs and 4 ML CdSe/3 ML CdS core/shells grown by colloidal atomic layer deposition below and above the ASE threshold. Reproduced from Ref. 41 with permission from the American Chemical Society. (c) All solution-cast vertical cavity laser of CQWs with 2 nm emission bandwidth. Reproduced from Ref. 88 with permission from the American Chemical Society. (d) Nanobeam photonic cavity used in continuous wave CQW laser operation with map of the field enhancement. Scale bars represent 500 nm. Reproduced from Ref. 35 with permission from Nature Publishing Group. (e) Room temperature gain spectrum of 4.5 ML CQWs under various excitation fluences. Reproduced from Ref. 102 with permission from The Royal Society of Chemistry. (f) Fluence-dependent emission of 5.5 ML CQW film at 80 K showing the emergence of ASE from the red feature of the photoemission. Reproduced from Ref. 34 with permission from the American Chemical Society.

simplest vertical cavity designs, which also have relatively wide spectra of multimodal lasing (4 to 6 nm) and lasing thresholds of 150–300 $\mu\text{J}\cdot\text{cm}^{-2}$ include vertical cavities formed by Bragg reflectors and silver mirrors.⁴² All solution-cast vertical cavity surface emitting lasers (VCSELs) have also been constructed with Bragg stacks using solution-deposition of alternating layers of silica and titania colloids (Figure 4c)⁹⁰ or two commercial reflectors⁹¹ under one- and two-photon excitation with somewhat improved bandwidth of 2–3 nm, which is nonetheless still multimodal. In one such VCSEL, room temperature CW lasing is reported at a threshold of 440 $\text{W}\cdot\text{cm}^{-2}$, which is remarkably low considering thresholds are more than 10 times higher for colloidal quantum dots.⁹³ Recently, whispering gallery lasers were demonstrated with coreless optical fibres, showing multimodal lasing thresholds of c. 190 $\mu\text{J}\cdot\text{cm}^{-2}$.¹⁰⁰ Continuous wave operation at a threshold of < 1 μW at room temperature was achieved in a high quality factor (linewidth < 0.2 nm) linear photonic crystal made through microfabrication.³⁵ The nanobeam cavity (shown in Figure 4d) enhances the spontaneous emission of photons into the cavity mode, reducing the threshold. Thus far, LED-like geometries with integrated distributed feedback cavities, considered the most promising route to electrically-pumped lasing in colloidal quantum dots,¹⁰¹ have not been demonstrated with CQWs.

B Mechanistic Aspects of Amplified Emission

As noted above, the properties of CQWs which are generally considered to explain their excellent performance as gain media are absence of inhomogeneous broadening, large cross-sections, large density of states, and slow Auger recombination. CQWs have much larger absorption cross-sections than for (smaller) semiconductor nanocrystals of the same composition. The linear absorption of CQWs scales with the lateral area for a given thickness of CQW and reported cross-sections at the band edge are c. $1\times 10^{-16}\text{ cm}^{-2}$ 2.5 ML,¹⁰² $5\times 10^{-14}\text{ cm}^{-2}$ for 4.5 ML, $1\times 10^{-14}\text{ cm}^{-2}$ for 5.5 ML.¹⁰³ The large density of states conferred by the atomically-precise CQWs narrows the spectral band of occupied states under population inversion. Unlike quantum dots, for which ensemble heterogeneity means that only a fraction of the sample has emission overlapping a given cavity mode, all of the CQW ensemble can participate.

Most reports indicate that ASE and lasing in CQWs are derived from the biexcitonic state, due to large exciton binding energies of CQWs from low dielectric environments, rather than an electron-hole plasma, as occurs in most epitaxial quantum wells including II-VI systems.^{104–106} The exciton binding energies of CQWs are estimated between 150–250 meV, with larger values for thinner CQWs.^{72,91,107} This biexcitonic emission is evidenced by a redshift from the single exciton fluorescence.^{42,91} In epitaxial systems, substantial gain occurs at high fluences (or currents) at which excitonic absorption is

bleached¹⁰⁸ and biexciton gain is observed only at lower temperatures, where weaker excitonic absorptions of epitaxial wells are preserved.¹⁰⁵ By contrast Figure 4e shows that excitonic absorptions are still observed at room temperature in CdSe CQWs for fluences of $>700 \mu\text{J}\cdot\text{cm}^{-2}$.¹⁰⁴ Recent work has suggested a reframing of the biexciton picture in favour of “excitonic molecules” in which multiexcitons can associate or dissociate.⁹⁷ The authors propose that a persistent population of dissociated excitons explains the simultaneous appearance of both optical gain and excitonic absorption.

Regardless, a critical aspect of gain in CQWs is competition with Auger relaxation. As-prepared, CQWs have long biexcitonic Auger relaxation times compared to quantum dots, reaching hundreds of picoseconds, chiefly due to larger separation of multiexcitons.^{83,87,89,109} Because non-radiative Auger competes with ASE, slow Auger processes permit longer gain lifetimes in CQWs.⁴² Data on volume-scaling of Auger relaxation in CQWs is conflicting. For quasi-spherical nanoparticles, Auger relaxation abides by linear volume scaling.¹¹⁰ In one report, CQWs showed essentially no change of biexcitonic Auger recombination time with lateral area at a given thickness;⁴² in another, the same parameter is said to vary linearly with volume and to the 7th power with thickness.¹⁰⁹ Auger recombination may be further slowed in core/shell geometries. CdSe/CdS CQWs made by colloidal ALD show non-monotonic growth in biexcitonic Auger relaxation times, which are longest (up to 700 ps) with 2-4 monolayer shells.¹¹¹ Growth of type II CdSe/CdTe core-crown structures also slows Auger recombination to as long as 1 ns and permits long gain lifetime through the spatial separation of charges.^{112,113} Use of graded interfaces, which suppress Auger in colloidal quantum dot core/shells, have not yet been demonstrated controllably for this application.

Several questions remain unresolved, including a complete picture of temperature-dependence, observations of electron-hole plasmas (if possible), or the influence of microstructure on optical gain. Sensitivity to temperature, and its influence on thresholds, modal gain coefficients and spectra, or the underlying photophysics of population-inverted samples have not been studied systematically. Lower thresholds are anticipated at lower temperatures, with temperature sensitivity intermediate between insensitive quantum dots¹¹⁴ and bulk materials.^{115,116} It is also reported that gain saturates at lower values at low temperature due to the giant oscillator effect,¹¹⁷ although direct measurements of absorption strength do not show substantial enhancement^{117,118} and measured exciton sizes are small.¹¹⁹ As an example of still unclear details of ASE in CQWs, Figure 4f shows emission of 5.5 ML CdSe CQWs at 80 K as a function of fluence: ASE emerges from the red emission feature, which has a disputed origin, not the band-edge emission feature.³⁴ At the same time, low-temperature gain spectra do not show any unusual behaviour in this respect.¹¹⁷ Another element which may contribute to the performance of CQW gain and lasing applications, but has not been investigated meaningfully, is the microstructure of CQW ensembles. Turbostratic disorder and its role in CQW lasing is not well-studied: it is speculated that highly-ordered CQW lamellae can cause parasitic scattering, but at the same time, permit higher

density and potentially higher gain coefficients.⁸⁶ Dipole alignment enforced by CQW stacking may reduce ASE or lasing thresholds by raising effective chromophore density.

6 Other Optoelectronics

A Transistors and Photodetectors

Similar to colloidal nanoparticles, transport measurements have been performed using arrays of CQWs. Use of arrays ensures relatively low mobility limited by charge transport from one CQW to the next, although the large lateral size of CQWs should permit single CQW devices. Presently, however, no equivalent to high electron mobility or modulation-doped electron transistors exists for CQWs.¹²⁰ A step toward single-CQW transport was made by draping CQWs over a well-defined 40-50 nm trench to prepare a transistor, although in this case, it still involves transport of many CQWs.¹²¹ Single CQW devices are very likely achievable, with potential similar to single nanowire or nanotube transistors. A larger barrier to realizing such devices is control over doping, either impurity or remote doping. Controlled modulation of carrier type in CQWs is limited to phototransistors of HgTe CQWs which have been made in both p-type and n-type using ethanedithiol and sodium sulphide capping ligand chemistry, respectively.¹²²

Arrays of CQWs in principle have advantages for transport compared with colloidal nanoparticles. CQW arrays have been used in transistors¹²³ and detectors.^{121,124,125} They can be paired with other two-dimensional materials or colloidal nanocrystals to manipulate charge or energy.¹²⁶⁻¹²⁸ Compared to quantum dot arrays, their larger size and high aspect ratios improve percolation.⁹ Their atomically-precise structure reduces site-energy dispersion, which should enable band-like transport and emergent electronic structure similar to epitaxial quantum wells¹²⁹ or close-packed colloidal nanoparticles¹³⁰⁻¹³² with appropriate control over the inter-CQW distance and the dielectric environment. Solids of stacked CQWs also open the possibility of excitonic transport via FRET, which is extremely fast in CQWs^{31,32} compared to other nanocrystals,¹³³ and even recently demonstrated to facilitate ASE.¹³⁴

In practice, reported electrolyte-gated thin-film transistor mobilities of CQW arrays are modest: 10^{-2} - $10^{-3} \text{ cm}^2\cdot\text{V}^{-1}\cdot\text{s}^{-1}$.¹²³ They do display very high on/off ratios, up to 10^8 , and sub-threshold slope of up to 78 mV per decade.¹³⁵ The greatest success has been the use of CQWs for detectors, which prize not only mobility, but also lifetime and extinction coefficient. Planar photodetectors, such as the figure 5a, and phototransistor geometries have been applied to both visible and short-wave infrared spectral ranges using CdSe, CdTe, or HgTe CQWs.^{9,122,124,125} Moving from a planar photodetector to a phototransistor geometry (with electrolyte gating) permits a large increase in photocurrent.¹²⁴ Short-wave IR detectors using HgTe/CdS CQWs show detectivity of 10^9 Jones driven in part by improvements in minority carrier lifetime compared to quantum dot analogues.¹²⁵ In current geometries, it remains unclear if CQWs can improve upon results with quasi-spherical nanocrystal.

B Electro-Optic Modulation

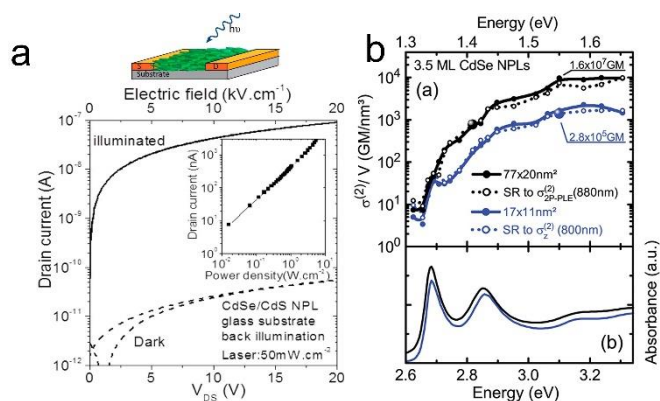


Figure 5. (a) CQW-based photodetector showing a large increase in photocurrent relative to dark current. Reproduced from Ref. 122 with permission from the American Chemical Society. (b) Two-photon absorption (top) as a function of energy and (bottom) linear absorbance of CdSe CQWs. Reproduced from Ref. 147 with permission from the American Chemical Society.

Modulation of absorption by electric fields (Stark effects) of quantum-confined nanostructures is substantially greater than in bulk materials, leading to what is termed the “quantum-confined Stark effect”.¹³⁶ The large, fast electroabsorption modulation of quantum well excitonic absorption in applied electric fields is a promising route toward modulating optical data transmission or developing optical interconnects.¹³⁷ In practice, static electric fields induce a bathochromic shift of quantum well excitonic absorption as well as a broadening of the absorption features weakening of absolute intensity.¹³⁸ The quantum-confined Stark effect is substantially stronger in CQWs than in nanorods or quantum dots.¹³⁹ In part, this is attributable larger exciton binding energies and the narrower bands of the CQW ensembles, which concentrate spectral changes in excitonic absorption, but it is also due to stronger dielectric screening in nanorods. The promise of CQWs for electroabsorption modulation (or electric-field modulation of photoluminescence)^{140,141} at the band edge is high. But further demonstration in thin films, particularly with CQWs in the NIR (below silicon bandgap) with controlled orientation using low voltages are important to access viability.

7 Non-Linear Optics

Epitaxial quantum wells are exploited in non-linear optical devices beyond gain media. Probably the most prominent use of nonlinear optics of epitaxial quantum wells exploits saturable absorption of excitons in mode-locked lasers, particularly integrated with Bragg reflectors in semiconductor saturable absorber mirror (SESAM) lasers, an important component in many pulsed laser systems.¹⁴² CQWs share the large cross sections and energetic structure which make epitaxial wells a preferred saturable absorber for these devices. The absence of substantial lateral carrier diffusion in CQWs (due to the finite lateral area) can slightly depress saturation intensities.^{143,144} There are a small number of investigations of CQWs as saturable absorbers.^{36,145,146} The reported saturation thresholds of CdSe CQWs range from 30-100 MW/cm², with increases for thicker CdS shells.^{145,146} When CdSe/CdS CQWs were placed on a silicon

nanobeam cavity, the cavity quality factor improved at higher fluences due to reduced absorption losses, demonstrating that this effect can be coupled to photonic architectures.³⁶ However, the large exciton binding energy of CQWs may also represent a liability in saturable absorption applications: the persistent excitonic absorption manifest in gain spectra (Figure 4e) diminishes the efficacy of saturable absorption. Prospects for core/shell species, which should reduce exciton binding energy through greater dielectric screening, in this application should be better.

Several works have examined the two-photon cross section of CQWs.^{146–150} These have found unusual superlinear volume scaling ($\propto V^2$) of two-photon absorption cross-sections, shown in Figure 5b for CdSe CQWs, as much as 10 times larger (10^7 GM) than other nanocrystals.¹⁴⁹ Such high two-photon cross sections suggest CQWs would be excellent candidates for two-photon imaging. This observation was subsequently explained based upon polarized two-photon absorption and theoretical analysis as deriving from spatially-correlated bound excitons—i.e. occupying a similar, smaller space than the boundaries of the CQW.¹⁴⁷ Similar to epitaxial quantum wells, CQWs have excitons smaller than the Bohr radius, close in size to the CQW thickness.^{119,129} The efficient two-photon absorption of CQWs has been employed in autocorrelation of sub-bandgap pulses, exploiting two-photon absorption detected by photoluminescence, with sensitivity up to 2 orders of magnitude higher than second harmonic detection with bulk materials (e.g. CdS).

Two areas of non-linear optics which have seen little treatment for CQWs—despite demonstrations with epitaxial quantum wells—are the characterization of CQWs for optical (AC) stark effects or frequency mixing processes. Optical Stark effects have been extensively studied in epitaxial wells,¹⁵¹ and recent works on other two-dimensional materials^{152,153} demonstrate that this effect can be exploited for optical switching or spintronics. Optical stark effects in CQWs are substantial and observed in experiments on using below band-gap excitation,¹⁵⁴ but they have not been mined for their fundamental insights or applications. Similarly, asymmetric epitaxial quantum wells have demonstrated efficacy for frequency mixing. For example second harmonic generation 1900 times more efficient than GaAs on resonance with the intersubband transitions (See next section) of asymmetric quantum wells.¹⁵⁵ Here, there remains a substantial barrier for CQWs: due to the symmetry of CQW synthesis there is presently no route to asymmetric wells.

8 Intersubband Applications

Despite the use of intersubband optical transitions of epitaxial quantum wells in quantum cascade lasers (QCLs)¹⁵⁶ and quantum well infrared photodetectors (QWIPs),¹⁵⁷ they have been sparingly-investigated in the case of CQWs. Both QCLs and QWIPs are unipolar devices which operate by exploiting the cascade of multi-quantum well energy states which occurs in an

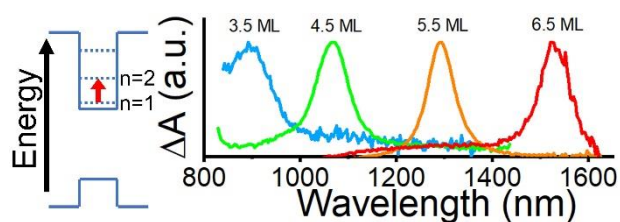


Figure 6. Cartoon showing intersubband transition between electron subbands and the spectroscopically observed intersubband transitions of CdSe CQWs of varying thickness. Data of change in absorbance are reported from transient absorption measurements under 400 nm pump excitation. Reproduced from Ref. 156 with permission from Nature Publishing Group.

applied electric field. In typical QCLs, electrons tunnel from the lowest subband ($n = 1$) energy level of one quantum well to a higher subband (e.g., $n = 2$) of the neighbouring quantum well, followed by photon emission, with the process repeated through the multi-well stack in a cascade.¹⁵⁶ In QWIPs, incident infrared photons resonant with intersubband transitions of the quantum wells enhance the photocurrent between emitter and collector terminals.¹⁵⁷

In epitaxial quantum well systems, these technologies are usually confined to the mid-IR and lower energies. Epitaxial materials with intersubband optical transitions in the near-IR or visible require very thin wells which are challenging to make with atomic precision. Not so colloidal quantum wells: polarized intersubband transitions of CdSe CQWs shown in Figure 6 occur from 900 nm to 1550 nm, tunable with thickness and temperature.¹⁵⁸ The bandwidth of these intersubband transitions is narrower (for this energy range) than some of the best examples based upon GaN and, for the thinnest samples, reaches higher energy than any reported epitaxial quantum well. Currently, intersubband absorptions are only observed in CdSe CQWs using transient absorption spectroscopy or spectroelectrochemistry because the ground state of the samples is undoped. The prospects for applying CQWs to these technologies are contingent on other challenges, such as electronic doping, modulation of barrier heights, inter-well spacing, and making effective electrical contact. But the key element—intersubband transitions in at much higher energy with narrow line-width—is in place to establish these technological possibilities. Use of colloidal material would relax constraints on the geometry of QWIPs and in the case of QCLs, the finite lateral size of CQWs may improve intraband relaxation such that QCLs become more efficient.¹⁴⁷

9 Prospects and Conclusions

The prospects of CQWs for many of the applications described in this review are *already* excellent: presently, no other materials offer the saturated colours or solution-processability which are so valuable in future downconversion films or LEDs. The high modal gain, large gain bandwidth, and long gain lifetimes of CQWs places CQWs in the company of materials such as III-V materials which are extensively used in mature laser technologies. This is true even though benefits from controlling film microstructure and alignment remain to be

mined fully. However, looming over much of these successes is the fact that most CQWs synthesized to date include toxic heavy metals (cadmium or mercury), and concerns about toxicity and encapsulation represent substantial barriers to use in commercial devices. This provides impetus to synthesis of non-toxic analogues, which is probably the largest advance to enable deployment of CQWs at large scale.

Many other optoelectronic applications of CQWs have not yet been the focus of sustained research. Some applications, such as electro-optic modulation, are probably straightforward to reach with controlled orientation of CQW deposition. In other areas, CQWs have all the essential properties, derived from their electronic structure, for exploitation in, for example, intersubband electronics or high-mobility transistors—but hitherto lack necessary accoutrements, such as control over doping. Synthetic elaborations to include doping, multi-well structures, or asymmetric CQWs would enable devices requiring emergent electronic structure (like QWIPs or QCLs) or uses in non-linear optics.

One drawback of this review's focus on technologies inherited from epitaxial quantum wells is that by design it does not cover new optoelectronic technologies exploiting the properties of CQWs, such as very large exciton binding energies, solution-processability, absence of inhomogeneous broadening, high quantum yields, or efficient FRET. For example, ease of integration of CQWs with other printing or patterning technologies opens possibilities for excitonic metasurfaces exploiting saturable absorption or electro-optic effects, which are much more challenging to fabricate with epitaxial wells. FRET-based transport of excitations may also enable efficient devices in films with classically poor transport. Another example may be optical refrigeration, which has been proposed for epitaxial quantum wells¹⁵⁹ but not practically implemented.

Although this review has covered only II-VI CQWs in detail, much of the essential physics and device opportunities apply to other atomically-precise two-dimensional colloids, such as perovskite plates^{160,161} or (as yet unrealized) III-V materials.. A few through lines are emphasized here. First, CQWs are excellent candidates for technologies which employ epitaxial quantum wells. In addition to potential advantages associated with low-cost deposition on arbitrary (including non-planar) substrates, CQWs offer in some cases opportunities to expand the spectral range and preserve narrower optical resonances than those achieved in epitaxial systems, especially very thin layers. Second, compared to other semiconductor nanocrystals the strength of inter-CQW interactions, particularly FRET, presents both new challenges and opportunities in device performance. Last, in many applications the performance of CQW devices has much unrealized potential for improvement achievable through controlled alignment. Aligning CQWs will take full advantage of their polarized electronic structure.

Conflicts of interest

There are no conflicts to declare.

Acknowledgements

This work was performed at the Center for Nanoscale Materials, a U.S. Department of Energy Office of Science User Facility, and supported by the U.S. Department of Energy, Office of Science, under Contract No. DE-AC02-06CH11357.

References

- S. Ithurria, M. D. Tessier, B. Mahler, R. P. S. M. Lobo, B. Dubertret and A. L. Efros, *Nat. Mater.*, 2011, **10**, 936–941.
- M. Nasilowski, B. Mahler, E. Lhuillier, S. Ithurria and B. Dubertret, *Chem. Rev.*, 2016, **116**, 10934–10982.
- E. Lhuillier, S. Pedetti, S. Ithurria, B. Nadal, H. Heuclin and B. Dubertret, *Acc. Chem. Res.*, 2015, **48**, 22–30.
- M. Sharma, S. Delikanli and H. V. Demir, *Proc. IEEE*, 2019, **PP**, 1–21.
- T. K. Kormilina, S. A. Cherevko, A. V. Fedorov and A. V. Baranov, *Small*, 2017, **13**, 1702300.
- C. Bouet, D. Laufer, B. Mahler, B. Nadal, H. Heuclin, S. Pedetti, G. Patriarcho and B. Dubertret, *Chem. Mater.*, 2014, **26**, 3002–3008.
- E. Izquierdo, A. Robin, S. Keuleyan, N. Lequeux, E. Lhuillier and S. Ithurria, *J. Am. Chem. Soc.*, 2016, **138**, 10496–10501.
- Y. Kelestemur, D. Dede, K. Gungor, C. F. Usanmaz, O. Erdem and H. V. Demir, *Chem. Mater.*, 2017, **29**, 4857–4865.
- S. Pedetti, B. Nadal, E. Lhuillier, B. Mahler, C. Bouet, B. Abécassis, X. Xu and B. Dubertret, *Chem. Mater.*, 2013, **25**, 2455–2462.
- M. Sharma, K. Gungor, A. Yeltik, M. Olutas, B. Guzelturk, Y. Kelestemur, T. Erdem, S. Delikanli, J. R. McBride and H. V. Demir, *Adv. Mater.*, 2017, **1700821**, 1–10.
- D. Chen, Y. Gao, Y. Chen, Y. Ren and X. Peng, *Nano Lett.*, 2015, **15**, 4477–4482.
- 10490624 B2, 2019.
- G. H. V. Bertrand, A. Polovitsyn, S. Christodoulou, A. H. Khan and I. Moreels, *Chem. Commun.*, 2016, **52**, 11975–11978.
- S. Pedetti, S. Ithurria, H. Heuclin, G. Patriarcho and B. Dubertret, *J. Am. Chem. Soc.*, 2014, **136**, 16430–16438.
- S. Ithurria and D. V. Talapin, *J. Am. Chem. Soc.*, 2012, **134**, 18585–18590.
- A. Hazarika, I. Fedin, L. Hong, J. Guo, V. Srivastava, W. Cho, I. Coropceanu, J. Portner, B. T. Diroll, J. P. Philbin, E. Rabani, R. Klie and D. V. Talapin, *J. Am. Chem. Soc.*, 2019, **141**, 13487–13496.
- B. Mahler, B. Nadal, C. Bouet, G. Patriarcho and B. Dubertret, *J. Am. Chem. Soc.*, 2012, **134**, 18591–18598.
- A. A. Rossinelli, A. Riedinger, P. Marqués-Gallego, P. N. Knusel, F. V. Antolinez and D. J. Norris, *Chem. Commun.*, 2017, **53**, 9938–9941.
- Y. Altintas, K. Gungor, Y. Gao, M. Sak, U. Quliyeva, G. Bappi, E. Mutlugun, E. H. Sargent and H. V. Demir, *ACS Nano*, 2019, **13**, 10662–10670.
- Y. Kelestemur, B. Guzelturk, O. Erdem, M. Olutas, K. Gungor and H. V. Demir, *Adv. Funct. Mater.*, 2016, **26**, 3570–3579.
- V. D. Jovanović, Z. Ikonić, D. Indjin, P. Harrison, V. Milanović and R. A. Soref, *J. Appl. Phys.*, 2003, **93**, 3194–3197.
- A. Antanovich, A. W. Achtstein, A. Matsukovich, A. Prudnikau, P. Bhaskar, V. Gurin, M. Molinari and M. Artemyev, *Nanoscale*, 2017, **9**, 18042–18053.
- B. T. Diroll and R. D. Schaller, *Chem. Mater.*, 2019, **31**, 3556–3563.
- M. Dufour, J. Qu, C. Greboval, C. Méthivier, E. Lhuillier and S. Ithurria, *ACS Nano*, 2019, **13**, 5326–5334.
- P. D. Cunningham, J. B. Souza, I. Fedin, C. She, B. Lee and D. V. Talapin, *ACS Nano*, 2016, **10**, 5769–5781.
- Y. Gao, M. C. Weidman and W. A. Tisdale, *Nano Lett.*, 2017, **17**, 3837–3843.
- E. Lhuillier, P. Hease, S. Ithurria and B. Dubertret, *Chem. Mater.*, 2014, **26**, 4514–4520.
- S. Shendre, S. Delikanli, M. Li, D. Dede, Z. Pan, S. T. Ha, Y. H. Fu, P. L. Hernández-Martínez, J. Yu, O. Erdem, A. I. Kuznetsov, C. Dang, T. C. Sum and H. V. Demir, *Nanoscale*, 2019, **11**, 301–310.
- S. Jana, M. de Frutos, P. Davidson and B. Abécassis, *Sci. Adv.*, 2017, **3**, e1701483.
- B. Abécassis, M. D. Tessier, P. Davidson and B. Dubertret, *Nano Lett.*, 2014, **14**, 710–715.
- C. E. Rowland, I. Fedin, H. Zhang, S. K. Gray, A. O. Govorov, D. V. Talapin and R. D. Schaller, *Nat. Mater.*, 2015, **14**, 484–489.
- B. Guzelturk, O. Erdem, M. Olutas, Y. Kelestemur and H. V. Demir, *ACS Nano*, 2014, **8**, 12524–12533.
- J. L. Movilla, J. Planelles and J. I. Climente, *ArXiv*, 2019, 1912.04182.
- B. T. Diroll, W. Cho, I. Coropceanu, S. M. Harvey, A. Brumberg, N. Holtgrewe, S. A. Crooker, M. R. Wasielewski, V. B. Prakapenka, D. V. Talapin and R. D. Schaller, *Nano Lett.*, 2018, **18**, 6948–6953.
- Z. Yang, M. Pelton, I. Fedin, D. V. Talapin and E. Waks, *Nat. Commun.*, 2017, **8**, 143.
- Z. Yang, M. Pelton and E. Waks, in *Conference on Lasers and Electro-Optics*, OSA, Washington, D.C., 2016, vol. 1, p. FF2B.4.
- S. Christodoulou, J. I. Climente, J. Planelles, R. Brescia, M. Prato, B. Martín-García, A. H. Khan and I. Moreels, *Nano Lett.*, 2018, **18**, 6248–6254.
- N. Hasanov, V. K. Sharma, P. L. Hernandez Martinez, S. T. Tan and H. V. Demir, *Opt. Lett.*, 2016, **41**, 2883.
- E. Beaudoin, P. Davidson, B. Abecassis, T. Bizien and D. Constantin, *Nanoscale*, 2017, **9**, 17371–17377.
- E. Beaudoin, B. Abecassis, D. Constantin, J. Degrouard and P. Davidson, *Chem. Commun.*, 2015, **51**, 4051–4054.
- M. D. Tessier, C. Javaux, I. Maksimovic, V. Lorette and B. Dubertret, *ACS Nano*, 2012, **6**, 6751–6758.
- C. She, I. Fedin, D. S. Dolzhenkov, P. D. Dahlberg, G. S. Engel, R. D. Schaller and D. V. Talapin, *ACS Nano*, 2015, **9**, 9475–9485.
- B. T. Diroll, D. V. Talapin and R. D. Schaller, *ACS Photonics*, 2017, **4**, 576–583.

- 44 M. D. Tessier, P. Spinicelli, D. Dupont, G. Patriarche, S. Ithurria and B. Dubertret, *Nano Lett.*, 2014, **14**, 207–213.
- 45 Y. Gao, M. Li, S. Delikanli, H. Zheng, B. Liu, C. Dang, T. C. Sum and H. V. Demir, *Nanoscale*, 2018, **10**, 9466–9475.
- 46 Y. Yang, C. Zhang, X. Qu, W. Zhang, M. Marus, B. Xu, K. Wang and X. W. Sun, *IEEE Trans. Nanotechnol.*, 2019, **18**, 220–225.
- 47 B. Liu, S. Delikanli, Y. Gao, D. Dede, K. Gungor and H. V. Demir, *Nano Energy*, 2018, **47**, 115–122.
- 48 Y. Altintas, U. Quliyeva, K. Gungor, O. Erdem, Y. Kelestemur, E. Mutlugun, M. V. Kovalenko and H. V. Demir, *Small*, 2019, **15**, 1804854.
- 49 R. Scott, J. Heckmann, A. V. Prudnikau, A. Antanovich, A. Mikhailov, N. Owschimikow, M. Artemyev, J. I. Climente, U. Woggon, N. B. Grosse and A. W. Achtstein, *Nat. Nanotechnol.*, 2017, **12**, 1155–1160.
- 50 E. Beaudoin, B. Abecassis, D. Constantin, J. Degrouard and P. Davidson, *Chem. Commun.*, 2015, **51**, 4051–4054.
- 51 D.-E. Yoon, W. D. Kim, D. Kim, D. Lee, S. Koh, W. K. Bae and D. C. Lee, *J. Phys. Chem. C*, 2017, **121**, 24837–24844.
- 52 L. D. Landau, E. M. Lifshits and L. P. Pitaevskii, *Electrodynamics of Continuous Media*, Pergamon, Oxford, 1st edn., 1960.
- 53 S. Coe-Sullivan, W. Liu, P. Allen and J. S. Steckel, *ECS J. Solid State Sci. Technol.*, 2012, **2**, R3026–R3030.
- 54 C. E. Rowland, I. Fedin, B. T. Diroll, Y. Liu, D. V. Talapin and R. D. Schaller, *J. Phys. Chem. Lett.*, 2018, **9**, 286–293.
- 55 A. Y. Kopusov, B. T. Spann, A. Bruma, P. Schuele, K. Bertness and A. Davydov, *J. Phys. Chem. C*, 2018, **122**, 5119–5123.
- 56 C. E. Rowland, W. Liu, D. C. Hannah, M. K. Y. Y. Chan, D. V. Talapin and R. D. Schaller, *ACS Nano*, 2014, **8**, 977–985.
- 57 C. E. Rowland and R. D. Schaller, *J. Phys. Chem. C*, 2013, **117**, 17337–17343.
- 58 B. T. Diroll and C. B. Murray, *ACS Nano*, 2014, **8**, 6466–6474.
- 59 Y. Zhao, C. Riemersma, F. Pietra, R. Koole, C. de M. Donegá and A. Meijerink, *ACS Nano*, 2012, **6**, 9058–9067.
- 60 O. Erdem, M. Olutas, B. Guzelurk, Y. Kelestemur and H. V. Demir, *J. Phys. Chem. Lett.*, 2016, **7**, 548–554.
- 61 H. D. Nelson, S. O. M. Hinterding, R. Fainblat, S. E. Creutz, X. Li and D. R. Gamelin, *J. Am. Chem. Soc.*, 2017, **139**, 6411–6421.
- 62 L. R. Bradshaw, K. E. Knowles, S. McDowall and D. R. Gamelin, *Nano Lett.*, 2015, **15**, 1315–1323.
- 63 X. Ma, B. T. Diroll, W. Cho, I. Fedin, R. D. Schaller, D. V. Talapin, S. K. Gray, G. P. Wiederrecht and D. J. Gosztola, *ACS Nano*, 2017, **11**, 9119–9127.
- 64 F. Feng, L. T. Nguyen, M. Nasilowski, B. Nadal, B. Dubertret, L. Coolen and A. Maître, *Nano Res.*, 2018, **11**, 3593–3602.
- 65 X. Ma, B. T. Diroll, W. Cho, I. Fedin, R. D. Schaller, D. V. Talapin and G. P. Wiederrecht, *Nano Lett.*, 2018, **18**, 4647–4652.
- 66 F. Feng, L. T. Nguyen, M. Nasilowski, B. Nadal, B. Dubertret, A. Maître and L. Coolen, *ACS Photonics*, 2018, **5**, 1994–1999.
- 67 R. M. Turtos, S. Gundacker, S. Omelkov, B. Mahler, A. H. Khan, J. Saaring, Z. Meng, A. Vasil'ev, C. Dujardin, M. Kirm, I. Moreels, E. Auffray and P. Lecoq, *npj 2D Mater. Appl.*, 2019, **3**, 1–10.
- 68 R. M. Turtos, S. Gundacker, S. Omelkov, E. Auffray and P. Lecoq, *J. Lumin.*, 2019, **215**, 116613.
- 69 R. M. Turtos, S. Gundacker, A. Polovitsyn, S. Christodoulou, M. Salomoni, E. Auffray, I. Moreels, P. Lecoq and J. Q. Grim, *J. Instrum.*, 2016, **11**, P10015–P10015.
- 70 L. A. Padilha, W. K. Bae, V. I. Klimov, J. M. Pietryga and R. D. Schaller, *Nano Lett.*, 2013, **13**, 925–932.
- 71 A. W. Achtstein, A. Schliwa, A. Prudnikau, M. Hardzei, M. V. Artemyev, C. Thomsen and U. Woggon, *Nano Lett.*, 2012, **12**, 3151–3157.
- 72 A. Naeem, F. Masia, S. Christodoulou, I. Moreels, P. Borri and W. Langbein, *Phys. Rev. B*, 2015, **91**, 8–12.
- 73 A. G. Vitukhnovsky, V. S. Lebedev, A. S. Selyukov, A. A. Vashchenko, R. B. Vasiliev and M. S. Sokolikova, *Chem. Phys. Lett.*, 2015, **619**, 185–188.
- 74 U. Giovanella, M. Pasini, M. Lorenzon, F. Galeotti, C. Lucchi, F. Meinardi, S. Luzzati, B. Dubertret and S. Brovelli, *Nano Lett.*, 2018, **18**, 3441–3448.
- 75 Z. Chen, B. Nadal, B. Mahler, H. Aubin and B. Dubertret, *Adv. Funct. Mater.*, 2014, **24**, 295–302.
- 76 P. Xiao, J. Huang, D. Yan, D. Luo, J. Yuan, B. Liu and D. Liang, *Materials (Basel)*, 2018, **11**, 1–22.
- 77 B. Liu, Y. Altintas, L. Wang, S. Shendre, M. Sharma, H. Sun, E. Mutlugun and H. V. Demir, *Adv. Mater.*, 2020, **32**, 1905824.
- 78 F. Zhang, S. Wang, L. Wang, Q. Lin, H. Shen, W. Cao, C. Yang, H. Wang, L. Yu, Z. Du, J. Xue and L. S. Li, *Nanoscale*, 2016, **8**, 12182–12188.
- 79 F. Fan, P. Kanjanaboos, M. Saravanapavanantham, E. Beauregard, G. Ingram, E. Yassitepe, M. M. Adachi, O. Voznyy, A. K. Johnston, G. Walters, G. H. Kim, Z. H. Lu and E. H. Sargent, *Nano Lett.*, 2015, **15**, 4611–4615.
- 80 B. Liu, M. Sharma, J. Yu, S. Shendre, C. Hettiarachchi, A. Sharma, A. Yeltik, L. Wang, H. Sun, C. Dang and H. V. Demir, *Small*, 2019, **15**, 1–9.
- 81 J. M. Pietryga, Y.-S. Park, J. Lim, A. F. Fidler, W. K. Bae, S. Brovelli and V. I. Klimov, *Chem. Rev.*, 2016, **116**, 10513–10622.
- 82 J. Kwak, W. K. Bae, D. Lee, I. Park, J. Lim, M. Park, H. Cho, H. Woo, D. Y. Yoon, K. Char, S. Lee and C. Lee, *Nano Lett.*, 2012, **12**, 2362–2366.
- 83 E. Baghani, S. K. O'Leary, I. Fedin, D. V. Talapin and M. Pelton, *J. Phys. Chem. Lett.*, 2015, **6**, 1032–1036.
- 84 D. Yokoyama, *J. Mater. Chem.*, 2011, **21**, 19187–19202.
- 85 Y. Arakawa and H. Sakaki, *Appl. Phys. Lett.*, 1982, **40**, 939–941.
- 86 M. Pelton, *J. Phys. Chem. C*, 2018, **122**, 10659–10674.
- 87 M. Pelton, S. Ithurria, R. D. Schaller, D. S. Dolzhenkov and D. V. Talapin, *Nano Lett.*, 2012, **12**, 6158–6163.
- 88 P. Sippel, W. Albrecht, J. C. Van Der Bok, R. J. A. Van Dijk-Moes, T. Hannappel, R. Eichberger and D. Vanmaekelbergh, *Nano Lett.*, 2015, **15**, 2409–2416.
- 89 C. She, I. Fedin, D. S. Dolzhenkov, A. Demortière, R. D. Schaller, M. Pelton and D. V. Talapin, *Nano Lett.*, 2014, **14**,

- 2772–2777.
- 90 B. Guzelturk, Y. Kelestemur, M. Olutas, S. Delikanli and H. V. Demir, *ACS Nano*, 2014, **8**, 6599–6605.
- 91 J. Q. Grim, S. Christodoulou, F. Di Stasio, R. Krahne, R. Cingolani, L. Manna and I. Moreels, *Nat. Nanotechnol.*, 2014, **9**, 891–895.
- 92 B. Guzelturk, M. Pelton, M. Olutas and H. V. Demir, *Nano Lett.*, 2019, **19**, 277–282.
- 93 F. Fan, O. Voznyy, R. P. Sabatini, K. T. Bicanic, M. M. Adachi, J. R. McBride, K. R. Reid, Y. Park, X. Li, A. Jain, R. Quintero-Bermudez, M. Saravanapavanantham, M. Liu, M. Korkusinski, P. Hawrylak, V. I. Klimov, S. J. Rosenthal, S. Hoogland and E. H. Sargent, *Nature*, 2017, **544**, 75–79.
- 94 M. Li, M. Zhi, H. Zhu, W.-Y. Y. Wu, Q.-H. H. Xu, M. H. Jhon and Y. Chan, *Nat. Commun.*, 2015, **6**, 1–8.
- 95 Y. Kelestemur, D. Dede, K. Gungor, C. F. Usanmaz, O. Erdem and H. V. Demir, *Chem. Mater.*, 2017, **29**, 4857–4865.
- 96 K. L. Shaklee and R. F. Leheny, *Appl. Phys. Lett.*, 1971, **18**, 475–477.
- 97 P. Geiregat, R. Tomar, K. Chen, S. Singh, J. M. Hodgkiss and Z. Hens, *J. Phys. Chem. Lett.*, 2019, **10**, 3637–3644.
- 98 A. V. Malko, A. A. Mikhailovsky, M. A. Petruska, J. A. Hollingsworth, H. Htoon, M. G. Bawendi and V. I. Klimov, *Appl. Phys. Lett.*, 2002, **81**, 1303–1305.
- 99 K. L. Shaklee, R. E. Nahory and R. F. Leheny, *J. Lumin.*, 1973, **7**, 284–309.
- 100 M. Sak, N. Taghipour, S. Delikanli, S. Shendre, I. Tanriover, S. Foroutan, Y. Gao, J. Yu, Z. Yanyan, S. Yoo, C. Dang and H. V. Demir, *Adv. Funct. Mater.*, 2020, **30**, 1–8.
- 101 J. Roh, Y. S. Park, J. Lim and V. I. Klimov, *Nat. Commun.*, 2020, **11**, 1–10.
- 102 S. Delikanli, G. Yu, A. Yeltik, S. Bose, T. Erdem, J. Yu, O. Erdem, M. Sharma, V. K. Sharma, U. Quliyeva, S. Shendre, C. Dang, D. H. Zhang, T. C. Sum, W. Fan and H. V. Demir, *Adv. Funct. Mater.*, 2019, **29**, 1901028.
- 103 A. Yeltik, S. Delikanli, M. Olutas, Y. Kelestemur, B. Guzelturk and H. V. Demir, *J. Phys. Chem. C*, 2015, **119**, 26768–26775.
- 104 Q. Li and T. Lian, *Chem. Sci.*, 2018, **9**, 728–734.
- 105 O. Homburg, P. Michler, R. Heinecke, J. Gutowski, H. Wenisch, M. Behringer and D. Hommel, *Phys. Rev. B*, 1999, **60**, 5743–5750.
- 106 F. P. Logue, P. Rees, J. F. Heffernan, C. Jordan, J. F. Donegan, J. Hegarty, F. Hiei, S. Taniguchi, T. Hino, K. Nakano and A. Ishibashi, *J. Opt. Soc. Am. B*, 1998, **15**, 1295.
- 107 S. J. Zelewski, K. C. Nawrot, A. Zak, M. Gladysiewicz, M. Nyk and R. Kudrawiec, *J. Phys. Chem. Lett.*, 2019, **10**, 3459–3464.
- 108 W. W. Chow, A. F. Wright, A. Girndt, F. Jahnke and S. W. Koch, *Appl. Phys. Lett.*, 1997, **71**, 2608–2610.
- 109 Q. Li and T. Lian, *Nano Lett.*, 2017, **17**, 3152–3158.
- 110 I. Robel, R. Gresback, U. Kortshagen, R. D. Schaller and V. I. Klimov, *Phys. Rev. Lett.*, 2009, **102**, 177404.
- 111 M. Pelton, J. J. Andrews, I. Fedin, D. V. Talapin, H. Leng and S. K. O’Leary, *Nano Lett.*, 2017, **17**, 6900–6906.
- 112 Q. Li, Z. Xu, J. R. McBride and T. Lian, *ACS Nano*, 2017, **11**, 2545–2553.
- 113 B. Guzelturk, Y. Kelestemur, M. Olutas, Q. Li, T. Lian and H. V. Demir, *J. Phys. Chem. Lett.*, 2017, **8**, 5317–5324.
- 114 I. Moreels, G. Rainaó, R. Gomes, Z. Hens, T. Stöferle and R. F. Mahrt, *Adv. Mater.*, 2012, **24**, 231–235.
- 115 H. Shoji, Y. Nakata, K. Mukai, Y. Sugiyama, M. Sugawara, N. Yokoyama and H. Ishikawa, *Appl. Phys. Lett.*, 1997, **71**, 193–195.
- 116 Y. Arakawa and H. Sakaki, *Appl. Phys. Lett.*, 1982, **40**, 939–941.
- 117 Q. Li, Q. Liu, R. D. Schaller and T. Lian, *J. Phys. Chem. Lett.*, 2019, **10**, 1624–1632.
- 118 B. T. Diroll, I. Fedin, P. Darancet, D. V. Talapin and R. D. Schaller, *J. Am. Chem. Soc.*, 2016, **138**, 11109–11112.
- 119 A. Brumberg, S. M. Harvey, J. P. Philbin, B. T. Diroll, B. Lee, S. A. Crooker, M. R. Wasielewski, E. Rabani and R. D. Schaller, *ACS Nano*, 2019, **13**, 8589–8596.
- 120 T. Mimura, S. Hiyamizu, T. Fujii and K. Nanbu, *Jpn. J. Appl. Phys.*, 1980, **19**, L225–L227.
- 121 E. Lhuillier, J. F. Dayen, D. O. Thomas, A. Robin, B. Doudin and B. Dubertret, *Nano Lett.*, 2015, **15**, 1736–1742.
- 122 C. Livache, E. Izquierdo, B. Martinez, M. Dufour, D. Pierucci, S. Keuleyan, H. Cruguel, L. Becerra, J. L. Fave, H. Aubin, A. Ouerghi, E. Lacaze, M. G. Silly, B. Dubertret, S. Ithurria and E. Lhuillier, *Nano Lett.*, 2017, **17**, 4067–4074.
- 123 E. Lhuillier, S. Pedetti, S. Ithurria, H. Heuclin, B. Nadal, A. Robin, G. Patriarche, N. Lequeux and B. Dubertret, *ACS Nano*, 2014, **8**, 3813–3820.
- 124 E. Lhuillier, A. Robin, S. Ithurria, H. Aubin and B. Dubertret, *Nano Lett.*, 2014, **14**, 2715–2719.
- 125 C. Gréboval, E. Izquierdo, C. Livache, B. Martinez, M. Dufour, N. Goubet, N. Moghaddam, J. Qu, A. Chu, J. Ramade, H. Aubin, H. Cruguel, M. Silly, E. Lhuillier and S. Ithurria, *Nanoscale*, 2019, **11**, 4061–4066.
- 126 N. Taghipour, P. L. H. Martinez, A. Ozden, M. Olutas, D. Dede, K. Gungor, O. Erdem, N. K. Perkgöz and H. V. Demir, *ACS Nano*, 2018, **12**, 8547–8554.
- 127 A. Robin, E. Lhuillier, X. Z. Xu, S. Ithurria, H. Aubin, A. Ouerghi and B. Dubertret, *Sci. Rep.*, 2016, **6**, 1–11.
- 128 A. Brumberg, B. T. Diroll, G. Nedelcu, M. E. Sykes, Y. Liu, S. M. Harvey, M. R. Wasielewski, M. V. Kovalenko and R. D. Schaller, *Nano Lett.*, 2018, **18**, 4771–4776.
- 129 D. A. B. Miller, in *Quantum Dynamics of Simple Systems*, eds. Oppo G.-L., S. M. Barnett, E. Riis and M. Wilkinson, Institute of Physics, London, 1996, pp. 239–266.
- 130 J.-H. Choi, A. T. Fafarman, S. J. Oh, D.-K. Ko, D. K. Kim, B. T. Diroll, S. Muramoto, J. G. G. Gillen, C. B. Murray and C. R. Kagan, *Nano Lett.*, 2012, **12**, 2631–2638.
- 131 J.-S. Lee, M. V. Kovalenko, J. Huang, D. S. Chung and D. V. Talapin, *Nat. Nanotechnol.*, 2011, **6**, 348–352.
- 132 X. Lan, M. Chen, M. H. Hudson, V. Kamysbayev, Y. Wang, P. Guyot-Sionnest and D. V. Talapin, *Nat. Mater.*, 2020, **19**, 323–330.
- 133 C. Kagan, C. C. Murray, M. Nirmal and M. Bawendi, *Phys. Rev. Lett.*, 1996, **76**, 1517–1520.
- 134 J. Yu, M. Sharma, A. Sharma, S. Delikanli, H. Volkan Demir and C. Dang, *Light Sci. Appl.*, 2020, **9**, 27.
- 135 E. Lhuillier, S. Ithurria, A. Descamps-Mandine, T. Douillard,

- 136 R. Castaing, X. Z. Xu, P. L. Taberna, P. Simon, H. Aubin and B. Dubertret, *J. Phys. Chem. C*, 2015, **119**, 21795–21799.
- D. A. B. Miller, D. S. Chemla, T. C. Damen, A. C. Gossard, W. Wiegmann, T. H. Wood and C. A. Burrus, *Phys. Rev. Lett.*, 1984, **53**, 2173–2176.
- 137 Y. H. Kuo, Y. K. Lee, Y. Ge, S. Ren, J. E. Roth, T. I. Kamins, D. A. B. Miller and J. S. Harris, *Nature*, 2005, **437**, 1334–1336.
- 138 N. V. Tepliakov, I. O. Ponomareva, M. Y. Leonov, A. V. Baranov, A. V. Fedorov and I. D. Rukhlenko, *J. Phys. Chem. C*, 2016, **120**, 2379–2385.
- 139 A. W. Achtstein, A. V. Prudnikau, M. V. Ermolenko, L. I. Gurinovich, S. V. Gaponenko, U. Woggon, A. V. Baranov, M. Y. Leonov, I. D. Rukhlenko, A. V. Fedorov and M. V. Artemyev, *ACS Nano*, 2014, **8**, 7678–7686.
- 140 R. Scott, A. W. Achtstein, A. V. Prudnikau, A. Antanovich, L. D. A. Siebbeles, M. Artemyev and U. Woggon, *Nano Lett.*, 2016, **16**, 6576–6583.
- 141 A. O. Muravitskaya, L. I. Gurinovich, A. V. Prudnikau, M. V. Artemyev and S. V. Gaponenko, *Opt. Spectrosc. (English Transl. Opt. i Spektrosk.)*, 2017, **122**, 83–87.
- 142 U. Keller, K. J. Weingarten, F. X. Kärtner, D. Kopf, B. Braun, I. D. Jung, R. Fluck, C. Hönninger, N. Matuschek and J. Aus Der Au, *IEEE J. Sel. Top. Quantum Electron.*, 1996, **2**, 435–451.
- 143 D. S. Chemla, A. C. Gossard, P. W. Smith, D. A. Miller and W. Wiegmann, *IEEE J. Quantum Electron.*, 1984, **20**, 265–275.
- 144 M. Kawase, E. Gannire, H. C. Lee and P. D. Dapkus, *IEEE J. Quantum Electron.*, 1994, **30**, 981–988.
- 145 A. M. Smirnov, E. V. Zharkova, A. D. Golinskaya, M. V. Kozlova, B. M. Saidzhonov, R. B. Vasiliev and V. S. Dneprovskii, in *Nonlinear Optics and Applications XI*, eds. M. Bertolotti and A. M. Zheltikov, SPIE, 2019, p. 14.
- 146 L.-B. Fang, W. Pan, S.-H. Zhong and W.-Z. Shen, *Chinese Phys. Lett.*, 2017, **34**, 098101.
- 147 J. Planelles, A. W. Achtstein, R. Scott, N. Owschimikow, U. Woggon and J. I. Climente, *ACS Photonics*, 2018, **5**, 3680–3688.
- 148 M. T. Quick, N. Owschimikow, A. H. Khan, A. Polovitsyn, I. Moreels, U. Woggon and A. W. Achtstein, *Nanoscale*, 2019, **11**, 17293–17300.
- 149 R. Scott, A. W. Achtstein, A. Prudnikau, A. Antanovich, S. Christodoulou, I. Moreels, M. Artemyev and U. Woggon, *Nano Lett.*, 2015, **15**, 4985–4992.
- 150 J. Heckmann, R. Scott, A. V. Prudnikau, A. Antanovich, N. Owschimikow, M. Artemyev, J. I. Climente, U. Woggon, N. B. Grosse and A. W. Achtstein, *Nano Lett.*, 2017, **17**, 6321–6329.
- 151 S. Schmitt-Rink, D. S. Chemla and D. A. B. Miller, *Adv. Phys.*, 1989, **38**, 89–188.
- 152 D. Giovanni, W. K. Chong, H. A. Dewi, K. Thirumal, I. Neogi, R. Ramesh, S. Mhaisalkar, N. Mathews and T. C. Sum, *Sci. Adv.*, 2016, **2**, 1–7.
- 153 E. J. Sie, J. W. McLver, Y. H. Lee, L. Fu, J. Kong and N. Gedik, *Nat. Mater.*, 2015, **14**, 290–294.
- 154 B. T. Diroll, P. Guo and R. D. Schaller, *Nano Lett.*, 2018, **18**, 7863–7869.
- 155 P. Boucaud, F. H. Julien, D. D. Yang, J. M. Lourtioz, E. Rosencher, P. Bois and J. Nagle, *Appl. Phys. Lett.*, 1990, **57**, 215–217.
- 156 J. Faist, F. Capasso, D. Sivco, C. Sirtori, A. L. Hutchinson and A. Y. Cho, *Science*, 1994, **264**, 553–556.
- 157 B. F. Levine, *J. Appl. Phys.*, 1993, **74**, R1–R81.
- 158 B. T. Diroll, M. Chen, I. Coropceanu, K. R. Williams, D. V. Talapin, P. Guyot-Sionnest and R. D. Schaller, *Nat. Commun.*, 2019, **10**, 4511.
- 159 J. Li, *Phys. Rev. B*, 2007, **75**, 155315.
- 160 M. C. Weidman, A. J. Goodman and W. a Tisdale, *Chem. Mater.*, 2017, **29**, 5019–5030.
- 161 Y. Bekenstein, B. A. Koscher, S. W. Eaton, P. Yang and A. P. Alivisatos, *J. Am. Chem. Soc.*, 2015, **137**, 16008–16011.

ARTICLE

Journal Name

The submitted manuscript has been created by UChicago Argonne, LLC, Operator of Argonne National Laboratory ("Argonne"). Argonne, a U.S. Department of Energy Office of Science laboratory, is operated under Contract No. DE-AC02-06CH11357. The U.S. Government retains for itself, and others acting on its behalf, a paid-up nonexclusive, irrevocable worldwide license in said article to reproduce, prepare derivative works, distribute copies to the public, and perform publicly and display publicly, by or on behalf on the Government. The Department of Energy will provide public access to these results of federally sponsored research in accordance with the DOE Public Access Plan. <http://energy.gov/downloads/doe-public-access-plan>.